Joint Report of PalMod Projects 989, 1030, and 1192

A. Overview

Due to significant cuts in the /work resources requested for 2026, production runs were repeatedly disrupted throughout the year. In particular, the CMORisation of the experiments required a great deal of /work. Nevertheless, we were able to carry out the majority of the experiments promised in the proposal.

Most of the positions of PalMod Phase III (Förderkennzeichen, FKZ) have finished as of the end of 2026; however, some projects will continue to run and analyse experiments through 2027 and into early 2028.

The funding of the project focused on the CMORisation of the data has also been completed (Project 1192); nevertheless, it is expected that data from experiments currently under evaluation will be archived in 2027.

For the references please see: https://www.palmod.de/publication-data/palmod_paper_06_26.pdf

B. Project: 989

Project title: PalMod WG1, Physical System

Project lead: Gerrit Lohmann (AWI), Gregor Knorr (AWI), Volker Klemann (GFZ), Uwe Mikolajewicz (MPI)

Report period: 2026-01-01 to 2026-10-31

1. Summary of work in 2026 at AWI

Overview

In the allocation period of 2026, the project focused on the continuation of simulations and on the analysis and publication of the simulations produced so far. Owing to the overall load on the HPC caused by the CMIP7 AFT production runs, part of the simulations planned for 2026 could not be completed; they are re-requested in the proposal for 2027. The work of the working group continued with the allocations granted for 2026; the remaining simulations are being completed and analysed by project scientists who continue to work on these topics.

Expired resources at the end of quarters I/II/III were unfortunately an issue. Over the year we have seen clear instances where simulations for which resources were allocated were not progressing, presumably due to the overall load on the HPC. From our point of view, expired resources are therefore linked to the fact that, owing to HPC congestion, simulations did not progress as planned.

Work at AWI

WP1.1: Multi-millennial future climate change scenarios

With the coupled AWI Earth System Model (AWI-ESM) including an interactive Greenland Ice Sheet (GrIS), the long-term evolution of the climate system under different future greenhouse gas scenarios was investigated until the year 4000 CE, with a focus on the interaction between the Atlantic Meridional Overturning Circulation (AMOC), Arctic sea ice and the GrIS. AMOC and Arctic sea ice respond comparatively fast to changes in radiative forcing and can recover partially or largely after a decline in greenhouse gas concentrations, whereas the GrIS responds with considerable delay owing to its long dynamic adjustment time: even after a rapid reduction of CO_2 concentrations following strong warming, substantial ice loss persists. In the high-emission scenarios, the simulated loss until 4000 CE corresponds to a global sea level rise of about 6 to 7.2 m. Meltwater inflow of more than 0.1 Sv does not trigger an AMOC collapse; decisive are the spatial distribution of the freshwater and its export from the North Atlantic. Long-term reversibility is thus not determined by the maximum warming alone, but by the ratio between the duration of the forcing and the adjustment times of the components. The study is under review at Communications Earth & Environment (preprint: https://doi.org/10.21203/rs.3.rs-8941071/v1). The results also contributed to the model intercomparison on the future evolution of the GrIS (Schannwell et al., 2026).

WP1.1 and WP1.2: Transient seamless trajectory simulations MIS3 to present-day

We have successfully completed a continuous transient simulation with the coupled climate-ice-sheet model AWI-ESM, from MIS 3 to the present-day (32 ka to 0 ka), using a temporal acceleration factor of 20 for testing and analysis. For the first time, our simulation provides a seamless trajectory into and out of the Last Glacial Maximum (~21 ka) and through the subsequent deglaciation, as well as the Holocene, capturing climate-ice-sheet coevolution across distinct climate states while closely matching available paleoclimate and sea-level records (Fig. 1a). In particular, we achieve an unprecedented reproduction of the sequential contribution of meltwater-pulse events to sea level changes, and identify the successive deglaciation of the Eurasian and North American ice sheets as their underlying source. A manuscript presenting these findings is in preparation for submission.

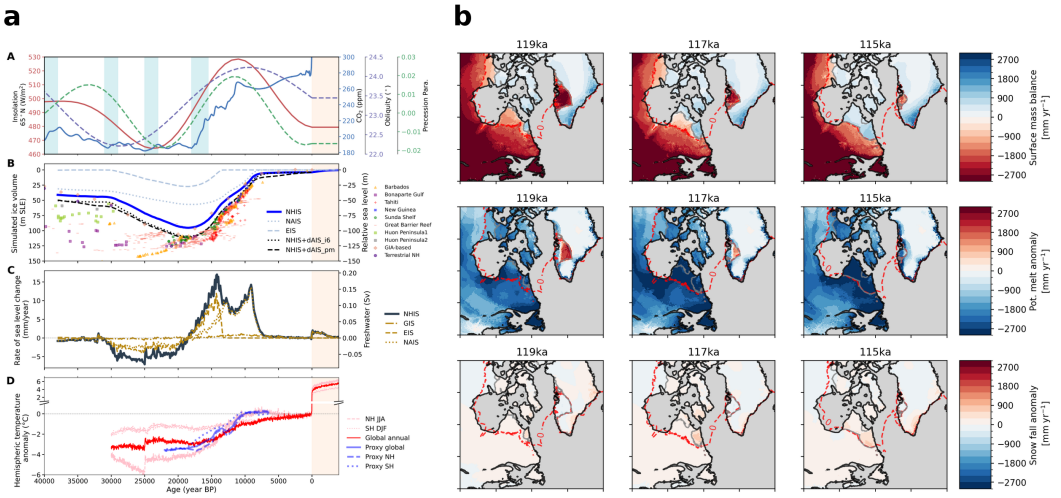


Figure 1: *(a) Insolation and CO_2 forcing, and simulated ice sheet-driven sea-level change and rate, and hemispheric surface temperature, compared with proxy reconstructions from 40,000 years ago into the*

future. (b) Anomalies of mean surface mass balance (top row), potential melt (middle row) and snow accumulation (bottom row) relative to the 12 ka climatology for 119 ka (left column), 117 ka (middle column) and 115 ka (right column).

WP1.3: Transient glacial inception

The transient simulation of the last glacial inception with AWI-ESM coupled to the Parallel Ice Sheet Model (PISM) was continued to about 55 ka BP and analysed. Between 127 ka and about 115 ka BP, initial glaciation is mainly controlled by a decrease in summer melt and follows the southward shift of the summer 0 °C isotherm (Fig. 1b). From about 115 ka BP onwards, growth increasingly continues independently of local climatic conditions: the ice-sheet margin advances into regions with negative local surface mass balance, made possible by the dynamic transport of ice from the accumulating interior (Fig. 2), while changes in moisture transport and in the snowfall fraction maintain a positive mass balance in the interior.

The results complement Niu et al. (2024), who highlight summer snowfall and the snow-albedo feedback for the growth of the Laurentide Ice Sheet between 38 and 20 ka BP, by showing that the dominant growth mechanisms already shift during the early glaciation phase. The comparison with the sea level stack of Spratt and Lisiecki (2016) places the simulated glaciation in the course of the last glacial cycle, although global sea level does not reflect the Laurentide Ice Sheet alone.

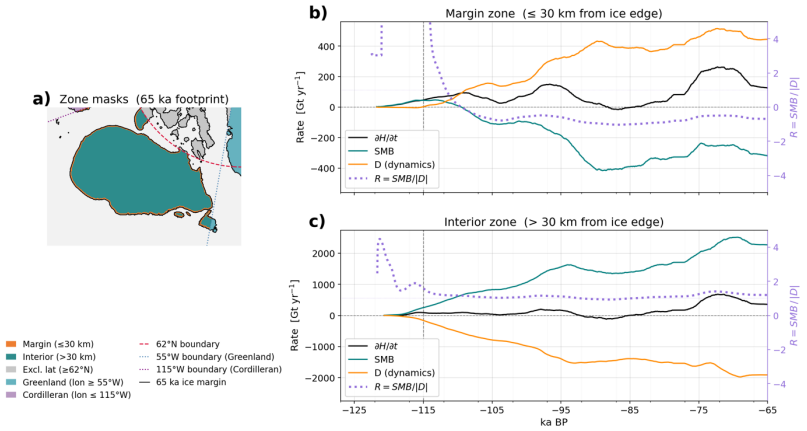


Figure 2: *Time series of the partitioning of the ice-sheet mass balance into surface mass balance (SMB) and a dynamic component (D), at the ice-sheet margin (within 30 km of areas with an ice thickness of more than 5 m; top right) and in the ice-sheet interior (bottom right), integrated over the area of the Laurentide Ice Sheet (left).*

The study has been submitted to the special issue “Understanding past climate variability to enhance future climate-change projections” of Climate of the Past (preprint: https://doi.org/10.5194/egusphere-2026-6177). Overall, glacial inception is not determined by orbital forcing and the resulting decrease in summer melt alone: with increasing ice-sheet size, ice dynamics and climatic feedbacks gain importance, which underlines the value of transient, coupled climate–ice sheet simulations.

WP3.2: Last deglaciation with isotope-enabled AWI-ESM2-WISO

During 2026, the main achievements were two isotope-enabled transient simulations of the last deglaciation (20–0 ka) using AWI-ESM2-WISO, based on the GLAC-1D and PaleoMIST ice-sheet reconstructions. Both simulations were performed with accelerated external boundary conditions (factor 5). In addition, two corresponding sensitivity experiments (noFWiso) were conducted, in

which the isotopic composition of prescribed meltwater was replaced by the local ocean isotopic composition. These paired experiments allow us to isolate the contribution of isotopically depleted glacial meltwater to simulated stable water isotope signals. Together, these four simulations represent approximately 16,000 AWI-ESM2-WISO model years of transient climate simulations.
The simulations reveal substantial differences in the climate and isotope responses associated with the two reconstructed meltwater histories (Fig. 3, left). GLAC-1D is characterized by pronounced freshwater pulses, particularly around 15–14 ka, accompanied by strong AMOC variability, with a substantial weakening followed by a rapid recovery and pronounced changes in Greenland surface temperature and precipitation $\delta^{18}O$. PaleoMIST, in contrast, exhibits a more gradual and sustained freshwater forcing with a relatively stable AMOC. Both simulations capture the overall deglacial warming and the broad evolution of Greenland precipitation $\delta^{18}O$ recorded in the NGRIP ice core.

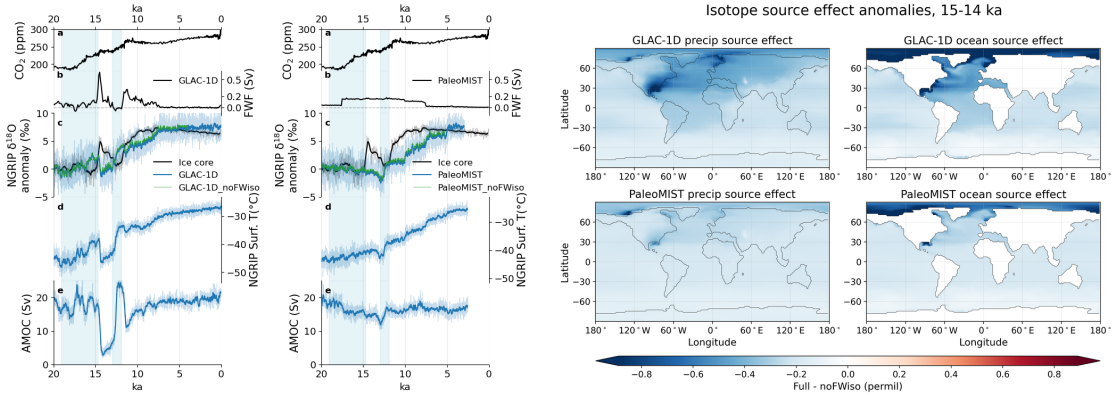


Figure 3: *Left: Deglacial evolution of climate and isotope variables in the GLAC-1D (left) and PaleoMIST (right) transient simulations. From top to bottom: atmospheric CO_2 concentration, freshwater forcing, Greenland precipitation $\delta^{18}O$ compared with the NGRIP ice-core record, Greenland surface temperature, and AMOC index. The green curves in the $\delta^{18}O$ panels represent the corresponding noFWiso sensitivity experiments. Right: Spatial distribution of the meltwater isotope source effect during 15–14 ka, calculated as the difference between the standard and noFWiso simulations. Results are shown for precipitation $\delta^{18}O$ (left) and surface-ocean $\delta^{18}O$ (right), using GLAC-1D (top) and PaleoMIST (bottom) ice-sheet reconstructions. Negative values indicate isotopic depletion associated with the prescribed glacial meltwater isotope composition.*
The sensitivity experiments show that meltwater isotope source effects depend strongly on the reconstructed freshwater history (Fig. 3, right). During 15–14 ka, GLAC-1D produces more pronounced negative isotope anomalies than PaleoMIST, particularly in precipitation $\delta^{18}O$ over Greenland and northern North America. Both simulations show a similar spatial pattern, with the strongest surface-ocean isotope depletion in the Arctic Ocean and Nordic Seas close to the meltwater input regions.

To test the implementation and impact of the interactive iceberg model (Ackermann et al., 2024), all four simulations are being repeated with the updated model configuration; they are expected to reach about 10 ka by the end of 2026, and the remaining integrations are planned for 2027.

2. Summary of work in 2026 at the MPI

A fully synchronously coupled simulation with the MPI-ESM-CR-mPISM-VILMA model system was performed with the focus on abrupt ice-sheet surges contributing to the climate variability over the MIS3 and part of the deglaciation period. The simulation from 55 ka to 15 ka shows millennial-

scale West-Antarctic icesheet instabilities with iceberg discharge magnitudes comparable to northern hemispheric Heinrich events during the last glacial period. Icebergs that are released from the Ross Sea follow two pathways: coastal release leads to westward transport and northward export through the iceberg alley in the Weddell Sea into the South Atlantic, while further off-shore release leads to eastward transport and melting in the Pacific Basin of the Southern Ocean. The melting of these discharged icebergs creates a global climate signature with a cooling in the extratropics of ~1 K in the Southern Hemisphere and ~0.5 K in the Northern Hemisphere. Furthermore, the concurrent stratification of the Southern Ocean reduces the ventilated volume in the Weddell Sea by ~62% and reduces the formation of Antarctic Bottom Water with a weakening of the bottom water cell in the South Atlantic from 4 to 2 Sv. In addition, a reduced meridional density gradient leads to a weakening of the Antarctic Circumpolar Current by approximately 50%. The potential occurrence of Southern hemispheric Heinrich events (SHEs) is supported from three independent sedimentary proxies: (i) ice-rafted debris, (ii) ACC reconstructions, and (iii) subglacial precipitates – all of which are consistent with the climatic signature of SHEs. This simulation suggests a more active role for the Antarctic ice sheet in shaping glacial climate variability than is commonly assumed. SHEs might be an additional source of glacial climate variability with a global climatic fingerprint, complementing established theories involving Dansgaard–Oeschger (DO) events, Heinrich events, and the bipolar seesaw mechanism (Schannwell et al, in review).

To investigate the stability of the Greenland Ice Sheet (GrIS), different sets of simulations have been carried out. Synchronously coupled simulation with the MPI-ESM-LR-mPISM-VILMA (higher spatial resolution and higher coupling frequency) show a substantial long-term decay of the GrIS as a consequence of future anthropogenic warming (Schannwell et al., in review, Kapsch et al., in review).

This raises the questions of whether critical thresholds of warming exist beyond which the complete loss of the GrIS is inevitable, and under what conditions a disappearance of the GrIS can be reversed.
As shown in Andernach et al. (2025), four stable states exist in MPI-ESM-CR-mPISM-VILMA under preindustrial CO2 forcing. Beside the present-day large state of the GrIS, we found three smaller stable states with approximately 50, 30 and 20% of the current ice volume. Quasi-steady state climate response simulations were performed with the MPI-ESM-CR-mPISM-VILMA to investigate the dependence of these stable states on the atmospheric greenhouse gas concentrations under slowly changing atmospheric CO2 concentrations (Fig.1.a).

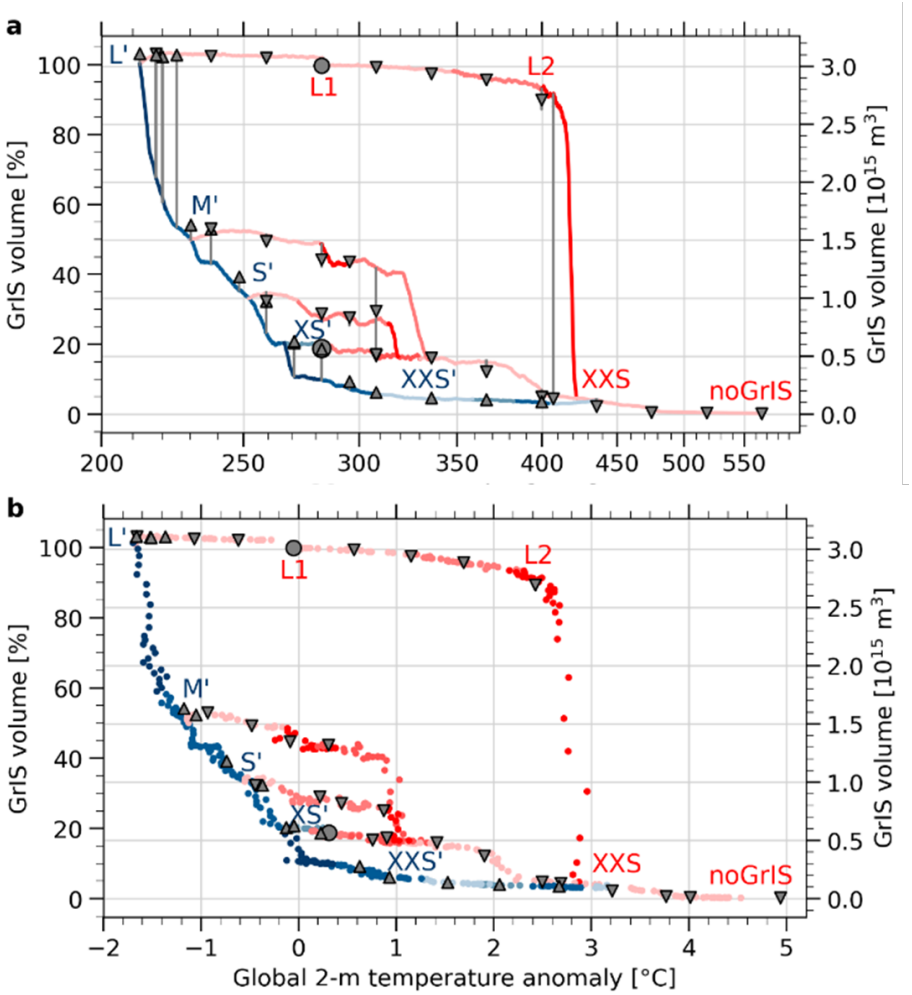


***Figure 1**: (a) Quasi-steady state response of the GrIS volume to CO2 forcing and (b) resulting global-mean 2-m temperature changes. Initial equilibrium states are shown as grey circles. Grey vertical lines in (a) show the trajectory of each equilibrium simulation and the triangles their end points: downward for retreat, upward for regrowth. Color shading indicates different forcing ramping directions (red: increasing, blue: decreasing) and speeds (darker: slower; fastest rate: 80,000 years for a CO2 doubling, i.e. much slower than observed CO2 changing rates)*

The present-day large state of the GrIS is quasi-stable with little mass loss until global warming reaches 2.55±0.15K (at 403±3.5 ppm) compared to the PI state. For higher temperatures, only a state with small ice caps on the mountains of East Greenland is stable, which also disappear under even higher temperatures. Cooling will allow for a stepwise regrowth of the disintegrated GrIS. However, even if the temperatures are reduced to a PI climate, the GrIS will only regrow to the smallest stable state with 20% of the PI ice volume. For a full regrowth, a cooling of 1.3±0.1K compared to PI is required (corresponding to 227.5±2.5 ppm). According to our simulations, we have already crossed the critical pCO2 threshold. If atmospheric CO2 levels are not reduced a practically irreversible long-term GrIS loss is triggered, Regrowth requires sustained CO2 reductions well below PI levels for tens to hundreds of thousands of years (Andernach et al., submitted).

3. Summary of work in 2026 Work at GFZ and PIK

In TP1 (GFZ), model runs at DKRZ continued to improve and verify the global 3D mantle viscosity structure for VILMA, in order to update the ensemble of Bagge et al. (2020). The resulting models are applied in TP2 (PIK) to improve the parameterisation of the Antarctic mantle structure and to investigate future projections. The sensitivity of present-day glacial changes to the underlying viscosity structure was investigated with a high-resolution ensemble of glacier responses over the last millennium (Fig. 5). In addition, code improvements regarding the rotational feedback and the convergence of the solution were made, and model runs for the current GIAMIP were performed.

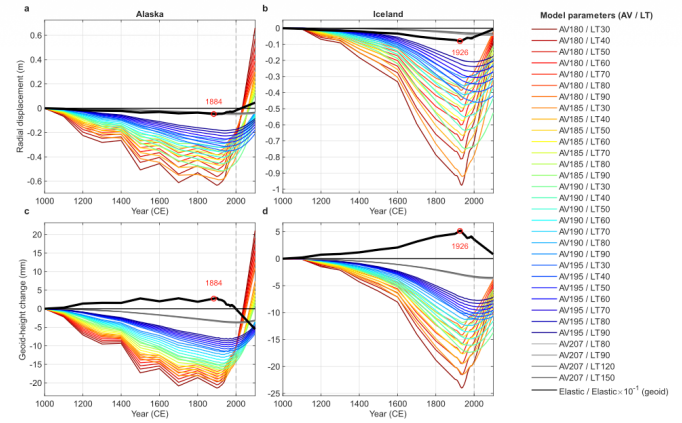


Figure 5: *Vertical deformation and geoid-height change driven by last-millennium glacier loading in Alaska and Iceland. Modelled radial displacement for Alaska (a) and Iceland (b) from 1000 to 2100 CE (negative values indicate subsidence). Modelled geoid-height change for Alaska (c) and Iceland (d); purely elastic response (black; scaled by ×10⁻¹ in c, d for clarity) and viscoelastic response in colours for different Earth structures (Sasgen et al., 2026).*

In TP2 (PIK), we performed PISM–VILMA simulations of the Antarctic Ice Sheet on centennial time scales at higher resolution than in the glacial-cycle simulations of Albrecht et al. (2024), based on the ISMIP6 extension experiments (Seroussi et al., 2024), in which feedbacks with the solid Earth and sea level had not been considered. Simulations from 1850 to 2300 with different climatic forcings and a range of 1D and 3D Earth structures quantify the delaying effect of the combined gravitational, rotational and deformational (GRD) response in VILMA on sea-level estimates (Fig. 6a); the results will be presented in Mojtabavi et al. (in prep.) and contributed to the GIA protocol for ISMIP7. The simulations were extended to the years 3000 and 12000 with climatic forcing from CLIMBER-X (Willeit et al., submitted; Fig. 6b).

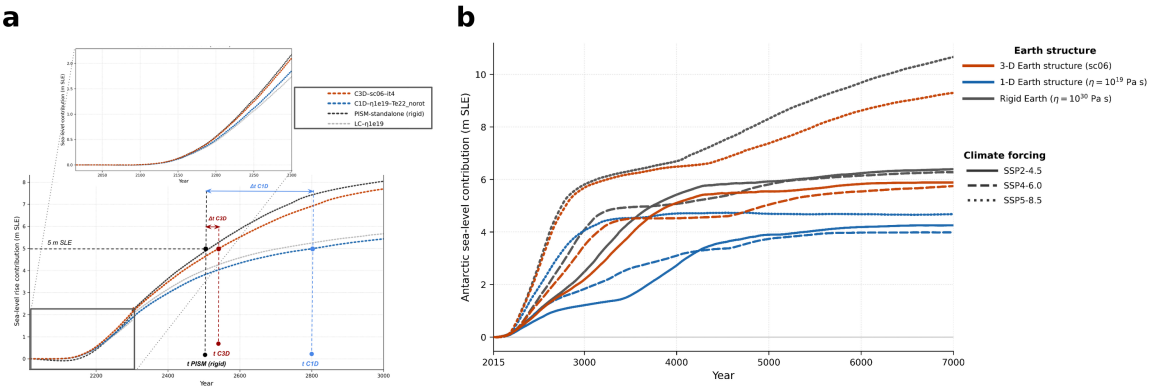


Figure 6: *(a) Comparison of Antarctic sea-level rise contributions from 2015 to 3000 for PISM-standalone, PISM-LC and PISM-VILMA with 3D Earth structure, forced with CESM2-WACCM under the high-emission scenario SSP5-8.5 using RACMO-derived surface mass balance; the sea-level feedback delays the contribution (preliminary). (b) Sea-level contributions from Antarctica in coupled PISM-VILMA simulations for three different Earth structures and three climate forcing scenarios until the year 7000.*

C. Project: 1030

Project title: PalMod WG2
Project lead: Victor Brovkin, Thomas Kleinen
Report period: 2026-01-01 to 2026-10-31

WG2 of PalMod aims at understanding and quantifying feedbacks between biogeochemistry and climate during glacial cycles. In PalMod Phase III, two work packages are focusing on the terrestrial and the marine carbon cycle.

WP2.1 "Terrestrial processes"investigates the feedbacks between climate and the terrestrial biosphere and carbon cycle for the entire last glacial cycle, with a major focus on the deglaciation and future climate. WP2.1 partner in this request is MPI-M.
WP2.2 "Marine processes" aims to improve the understanding of feedbacks between ocean biogeochemistry and climate for the last deglaciation and thereby improve the skills of ESMs in projecting the future ocean carbon sink and the changes in the marine environment. WP2.2 partners in this request are AWI, CAU Kiel and UHH.

1. Summary of work in 2026 in WP2.1 "Terrestrial Processes", MPI-M

WP2.1 performs work in three areas: 1) Transient modelling of the coupled global carbon cycle, 2) analysis of land cover changes in model and reconstructions, and 3) the role of remobilised permafrost carbon during the deglaciation.

For our study of the global carbon budget over glaciation cycles, we had previously completed all simulations, and over the course of 2026 we post-processed much of the model output and summarized our results in a manuscript that has already been submitted and is currently under review.
In this study we collaborated with WP1.1, who provided us with simulations of the last deglaciation with interactive ice sheets. Our main finding is that the contribution of land cover to rising greenhouse gases in the atmosphere happens on two timescales, as it responds to either slower orbital parameter variations, or faster meltwater release from ice-sheet decay. We show that terrestrial processes can explain both long-term and short-term signals in ice-core records of atmospheric greenhouse gases during glacial cycles.
Figure 2.1-1 highlights the land fast carbon exchanges with the atmosphere, across the northern tropical band, where meltwater release events during the deglaciation induce sudden changes in precipitation patterns that result in fast land cover changes and concomitant carbon emissions.

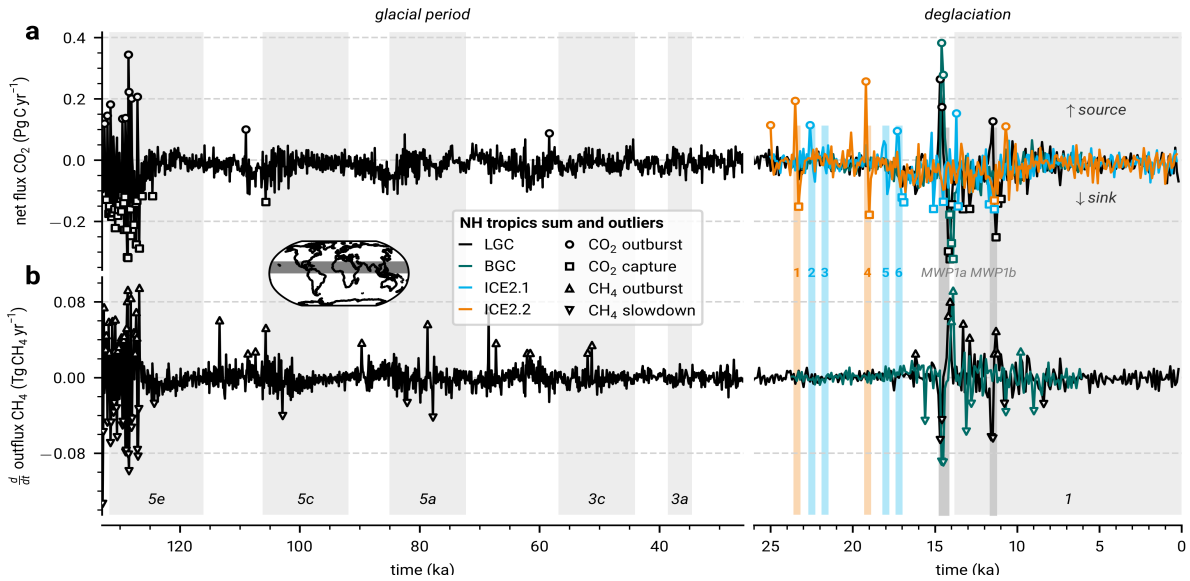


Fig. 2.1-1: Fast carbon transfers from land GHG emissions within the tropical Northern Hemisphere from: (a) net flux of CO2 and (b) the time derivative of the net CH4 emissions. Experiments named LGC, BGC, ICE2.1 and ICE2.2 cover different periods. Outliers are detected using z-scores of the median of absolute deviations from the median. Vertical shades highlight marine isotopic stages and meltwater release in the North Atlantic.

In 2026 we have continued to investigate the role of remobilised permafrost carbon on atmospheric CO_2 during the deglaciation; particularly on abrupt rises in CO_2 concentrations. We have run several simulations (with various different assumptions used in the model and initialisation) of the last deglaciation with MPI-ESM including a permafrost model initialised with carbon inventory from Lindgren et al 2025. Analysis of these simulations have shown that approximately 150-175 PgC of frozen carbon are thawed and released to the atmosphere during the 18ka-11ka BP period in our model, given the initial stocks in the Lindgren et al dataset. About 20 Pg of frozen carbon are also lost during the flooding of continental shelves as the land-sea mask changes; the fate of this flooded shelf carbon is unclear. An abrupt release of permafrost carbon is observed around 14ka BP where about 40 Pg of carbon is release across the course of a few hundred years. This is caused by a sudden rise in 2-meter temperatures across the north Atlantic/arctic ocean in our simulation at this point, possibly related to changes in the MOC.

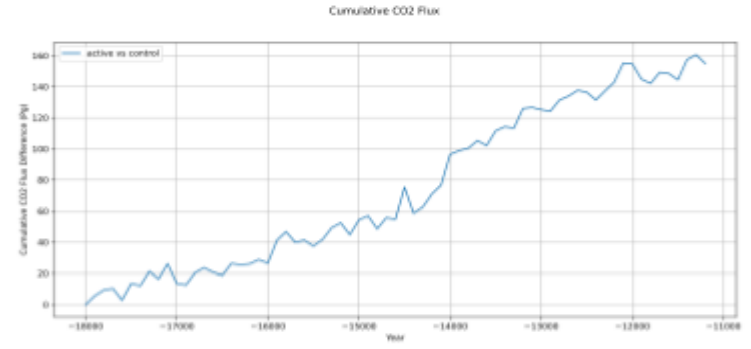


Figure 2.1-3: Difference to CO2 Flux to the atmosphere with and without the Permafrost model from MPI-ESM transient simulations.

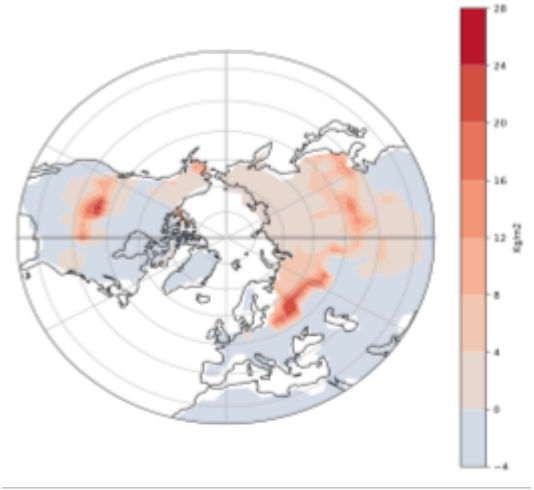


Figure 2.1-4: Thawed permafrost release between 18-11ka BP in MPI-ESM transient experiments.

2. Summary of work in 2026 in WP 2.2 “Marine processes“, CAU Kiel

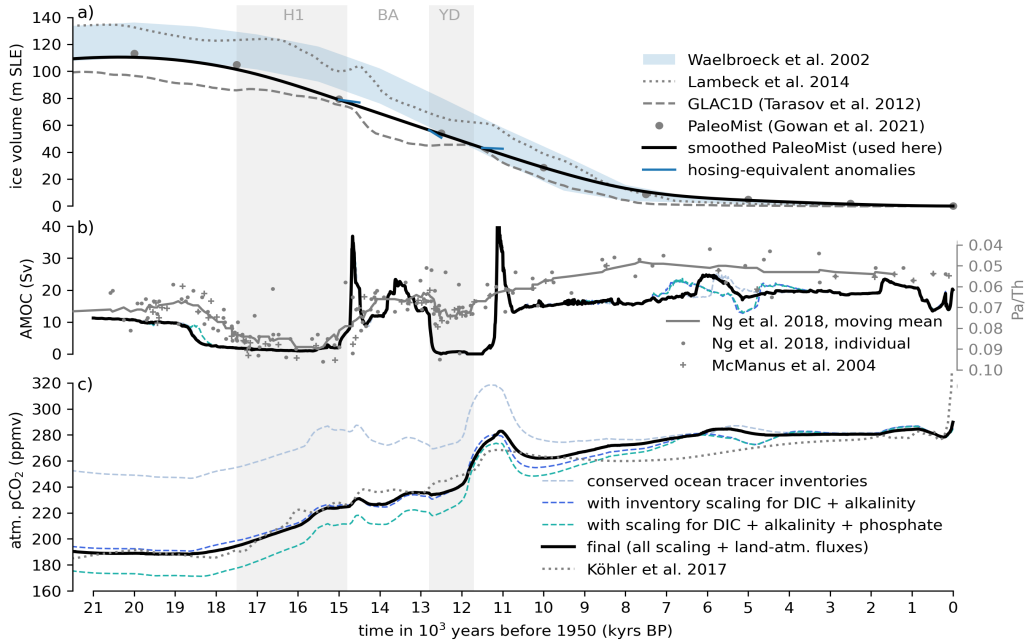


Fig. 2.2-1: Simulations of the last deglaciation with conserved ocean tracer inventories and with scaled alkalinity, dissolved inorganic carbon (DIC) and phosphate inventories, as we originally planned for MPI-ESM, here shown for CLIMBER-X. a) Simulated ice volume (black) in meters sea-level equivalent (m SLE) compared to ice volume and sea-level reconstructions. b) Simulated Atlantic meridional overturning circulation (AMOC); to achieve AMOC recoveries in line with Pa-Th paleo-reconstructions (grey), negative freshwater “hosing” is applied (short blue lines in panel a. c) Simulated atmospheric pCO_2 compared to ice-core based reconstructions (dashed grey line, Köhler et al. 2017).

For 2026 we had originally planned to run a total of 4 transient deglaciation simulations with MPI-ESM (2 simulations with different freshwater forcing and 2 sensitivity runs with scaled alkalinity,

DIC and nutrient inventories to test the shelf hypothesis). Unfortunately, we were not able to do these runs due to the prioritization of CLIMBER-X simulations (Fig. 2.2-1). Most of our CLIMBER-X simulations were run on the local cluster at CAU Kiel. Therefore, we hardly used any of the 48000 requested / ~21000 granted node hours.

The 168 node hours accounted to date were used to run CLIMBER-X PI spinups with reduced ocean and biogeochemistry timestep, and parts of transient deglaciation simulations at a time when computational resources at CAU Kiel were limited. At least one of the PI spinups will likely be used in a publication on transient deglaciation simulations with CLIMBER-X that is currently in preparation.

3. Summary of work in 2026 in WP 2.2 "Marine processes", UHH

We have conducted further LGM simulations with MPI-ESM1.2 to examine how different glacial boundary conditions affect glacial ocean carbon sequestration. We've also conducted idealised simulations, in which marine biological production is switched off, to disentangle the impacts of ocean physics and marine productivity on glacial-interglacial atmospheric CO2 changes (Fig. 2.2-2). These simulations have supported the manuscript's multi-model comparison of the glacial ocean carbon cycle (Liu et al., submitted). We are currently conducting transient deglacial simulations with marine biology switched off to isolate the impact of deglacial changes in ocean circulation and biological production on atmospheric CO2 variations.

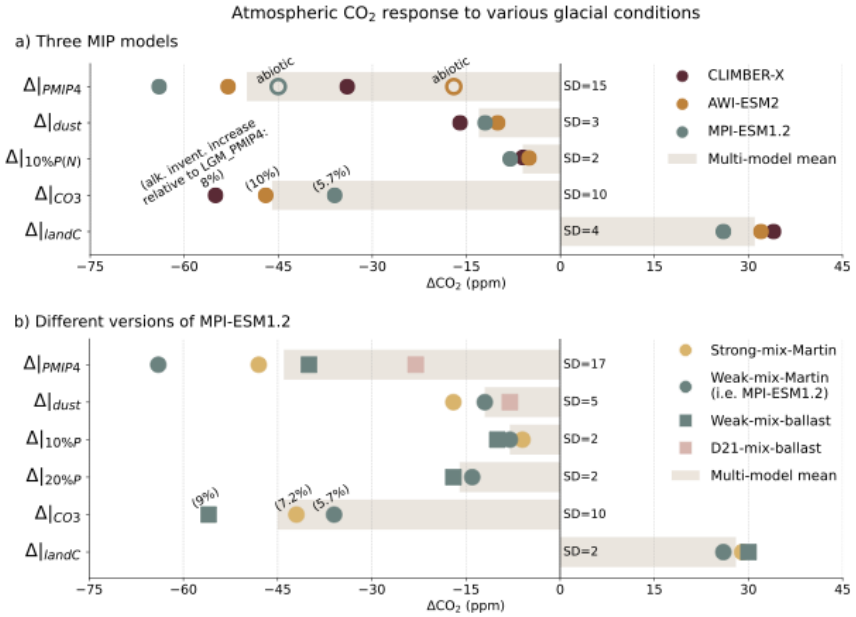


Fig. 2.2-2: Atmospheric CO2 changes in response to the PMIP4 LGM boundary conditions, glacial dust deposition, increased glacial oceanic nutrient inventory, CO3 compensation and 500 GtC glacial terrestrial carbon release in (a) three PalMod models (CLIMBER-X, AWI-ESM2, MPI-ESM1.2) and (b) in different versions of MPI-ESM1.2.

4. Summary of work in 2026 in WP2.2 “Marine processes“, AWI Bremerhaven

In 2026, the work at AWI focused on tuning the new model version (AWI-ESM2 with the new FESOM version) and adding new processes, to prepare future scenario simulations. From January to October 2026, these simulations used 87525 node hours. Because the project had low priority on levante, this took considerably longer than expected. Since August in particular, long queue times have cut our use of computing resources to about one fifth of what we planned.

The work included:

1. Tuning of the physical ocean. The new tuning improved the meridional overturning circulation (MOC) under PI conditions, reduced the warm bias over the Southern Ocean and the too large Weddell Sea polynya (Fig. 1).
2. Iron cycle response to climate change. To better represent how the iron cycle responds to future climate change (prepared for the future scenarios), we implemented a pH- and DOC-dependent parameterisation of iron–ligand binding (Ye et al. 2020). It was applied in PI simulations, tuned and compared with GEOTRACES data.
3. Changing iron sources. To better capture how climate change alters iron supply, we added ice-shelf and iceberg melting as iron sources that are sensitive to future warming. Preliminary results show that this additional iron source substantially increases productivity (Fig. 2, Tian et al. 2026).

Existing PI. LGM and hosing simulations have been analysed and used in the recent submission to the PalMod special issue in Climate of the Past (Ye et al. submitted). New reference simulations under PI and LGM conditions are still being analysed.

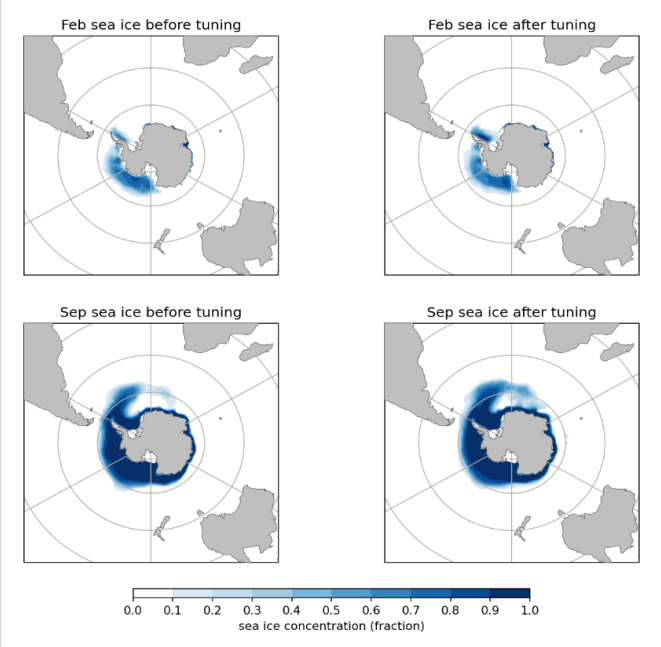


Figure 1 Sea ice concentration during February and September before and after tuning work in PI simulations.

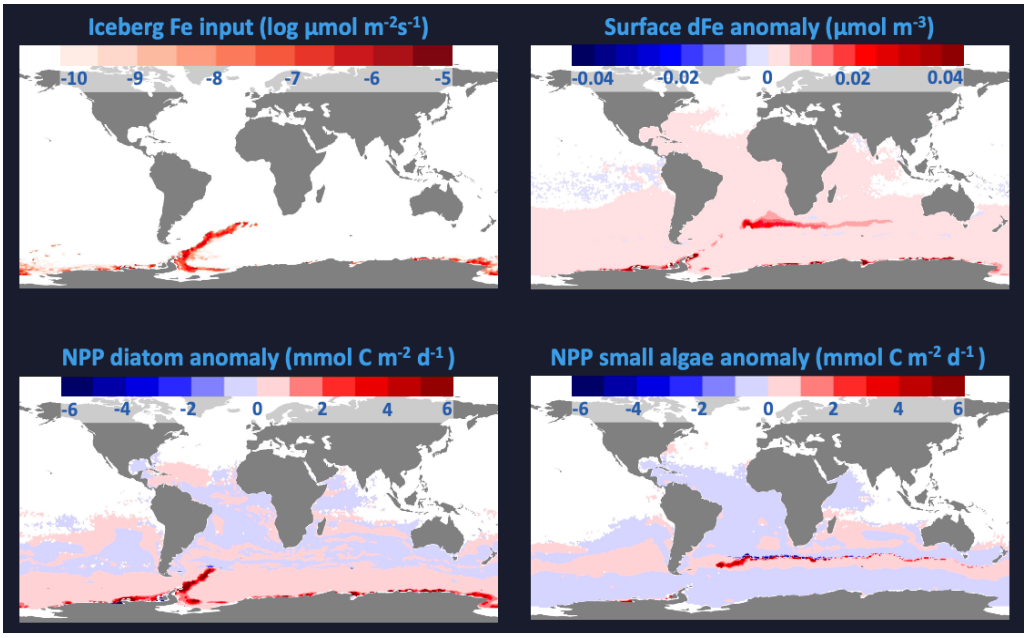


Figure 2 Anomaly in iron source, surface iron concentration and primary productivity by diatom and small phytoplankton in response to changes in iron input.

D. Project: 1192

Project title: PalMod Data Project
Project lead: Swati Gehlot
Report period: 2026-01-01 to 2026-10-31

Summary of work in 2026

To make a large consortium project like PalMod successful, it needs to take care for efficient data exchange between project partners and also with external partners. Therefore, the project bk1192 was the platform for establishing a framework enabling efficient, timely, and low barrier data exchange. This is necessary because there is an articulated need for improved intra-project collaboration and because storage space on /work is limited.
A workflow and a recipe detailing the import, access, share and distribute the data via the common data pool supplied by bk1192 was developed (and distributed PalMod-wide) in close collaboration with the scientists with respect to their concrete requirements in the year 2025-2026. Along with being a core space for internal data sharing within the PalMod scientific WGs, the data pool bk1192 is also a dedicated space for DataHub-CC1 development and extension of model specific CMORization and publication workflows. Figure 1 shows the systematic usage plan of bk1192 for inflow and outflow of PalMod data.

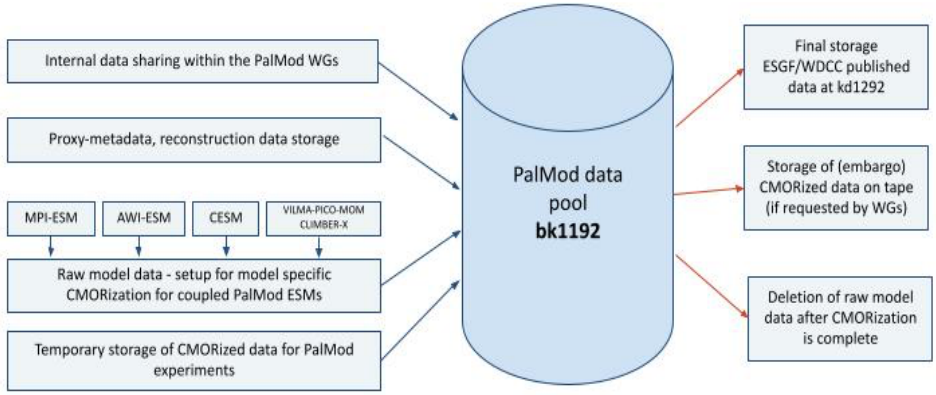


Figure 1: *Storage workflow for PalMod data pool bk1192 resource. The multiple sources of data input are shown with blue arrows. The red arrows show the subsequent movement of data after the CMORization is completed for coupled ESMs*.

Since the first allocation of space bk1192 in early 2021 (105TB available each for /work and /arch), the PalMod data pool continues to build up and grow in storage with the shared data from project partners (currently using ~86TB, with more data (~ 170 TB via MPI-ESM models) during the year for CMOR storage). The table below lists the current overview of storage of shared data at bk1192.

Overview storage space for the data project bk1192

Working Group/ Work package	**Lustre work [TB]**
WG 1/ WP 1.1 (MPI-ESM)	0
WG 1/ WP 1.4 (VILMA)	0.068
WG 2/ WP 2.1 (MPI-ESM)	9.1
WG 2 /WP 2.3 (MPI-ESM)	6.1
WG 3/ WG 3.2	0.0004
WG 1/ WP 1.1 (MPI-ESM) - v2/v3	~72 (170 TB tmp. during CMOR til 10/26)
WG 1/ WP 1.2 (AWI-ESM)	10
CMORized data storage (temp.)	0
Total used	**~ 97.2**

Since August 2021, the PalMod data pool is used as a primary resource for development of model specific CMORization, ESGF publication and WDCC archiving workflows within PalMod-II, and to be extended towards Palmod-III. Currently the test setups consist of data from all the three coupled PalMod ESMs.

Three sets of PalMod experiments for MPI-ESM were published on DKRZ ESGF portal (https://esgf-data.dkrz.de/search/palmod/) in 2022-23.
These ESGF published simulations comprised of MPI-ESM transient simulations in Kapsch et al., 2022, (https://doi.org/10.1029/2021GL096767), MPI-ESM transient deglaciation runs with Methane Future Scenarios in Kleinen et al, 2021 (doi:10.1088/1748-9326/ac1814), and MPI-ESM transient Deglaciation interactive in Mikolajewicz et al, 2025 (https://doi.org/10.5194/cp-21-719-2025).
The final set of CMORized data is stored at dedicated long term PalMod tape resource (kd1292), along with a backup on bk1192 tape resources and via long term archival via WDCC (World Data Centre for Climate) at https://www.wdc-climate.de/ui/project?acronym=PalMod2 .

The future transient scenario runs (MPI-ESM v2/v3, M.Kapsch, MPI) are CMORized and kept embargo currently. These datasets will be published via WDCC with data DOI together with the manuscript publication (expected in the last quarter of 2026).

PalMod DataHub CC1 developed a project-wide strategy for the long-term preservation and accessibility of project data to fulfil the funder requirements and also facilitate data reuse beyond the PalMod consortium and influence the layout of project bk1192. In addition to supporting the data management activities for PalMod-II, the data pool bk1192 also acted as a platform for building up the prerequisite basis for continuing towards PalMod Phase-III.